

Giant enhancement of reflectance due to the interplay between surface confined wave modes and nonlinear gain in dielectric media

SANGBUM KIM AND KIHONG KIM*

Department of Energy Systems Research and Department of Physics, Ajou University, Suwon 16499, Korea

*khkim@ajou.ac.kr

Abstract: We study theoretically the interplay between the surface confined wave modes and the linear and nonlinear gain of the dielectric layer in the Otto configuration. The surface confined wave modes such as surface plasmons or waveguide modes are excited in the dielectric-metal bilayer by obliquely incident p waves. In the purely linear case, we find that the interplay between linear gain and surface confined wave modes can generate a large reflectance peak with its value much greater than 1. As the linear gain parameter increases, the peak appears at smaller incident angles, and the associated modes also change from surface plasmons to waveguide modes. When the nonlinear gain is turned on, the reflectance shows very strong multistability near the incident angles associated with surface confined wave modes. As the nonlinear gain parameter is varied, the reflectance curve undergoes complicated topological changes and sometimes displays separated closed curves. When the nonlinear gain parameter takes an optimally small value, a giant amplification of the reflectance by three orders of magnitude occurs near the incident angle associated with a waveguide mode. We also find that there exists a range of the incident angle where the wave is dissipated rather than amplified even in the presence of gain. We suggest that this can provide the basis for a possible new technology for thermal control in the subwavelength scale.

© 2018 Optical Society of America

OCIS codes: (190.1450) Bistability; (190.5940) Self-action effects; (240.4350) Nonlinear optics at surfaces; (240.6680) Surface plasmons.

References and links

1. J. Homola, S. S. Yee, and G. Gauglitz, "Surface plasmon resonance sensors: review," *Sens. Actuators, B* **54**(1–2), 3–15 (1999).
2. K. Kneipp, H. Kneipp, I. Itzkan, R. R. Dasari, and M. S. Feld, "Surface enhanced Raman scattering and biophysics," *J. Phys.: Condens. Matter* **14**(18), R597–R624 (2002).
3. I. Pockrand, J. D. Swalen, J. G. Gordon II, and M. R. Philpott, "Surface plasmon spectroscopy of organic monolayer assemblies," *Surf. Sci.* **74**(1), 237–244 (1977).
4. B. Liedberg, C. Nylander, and I. Lunström, "Surface plasmon resonance for gas detection and biosensing," *Sens. Actuators* **4**, 299–304 (1983).
5. T. Okamoto and I. Yamaguchi "A surface plasmon microscope," *Proc. SPIE* **1319**, 472–473 (1990).
6. P. T. Leung, D. Pollard-Knight, G. P. Malan, and M. F. Finlan, "Modelling of particle-enhanced sensitivity of the surface-plasmon-resonance biosensor," *Sens. Actuators, B* **22**(3), 175–180 (1994).
7. E. M. Yeatman, "Resolution and sensitivity in surface plasmon microscopy and sensing," *Biosens. Bioelectron.* **11**(6–7), 635–649 (1996).
8. P. Törmä and W. L. Barnes, "Strong coupling between surface plasmon polaritons and emitters: a review," *Rep. Prog. Phys.* **78**(1), 013901 (2015).
9. M. I. Stockman, "Net optical gain in a plasmonic waveguide embedded in a fluorescent polymer," *Nat. Photon.* **4**(7), 457–461 (2010).
10. M. I. Stockman, "Amplification of long-range surface plasmons by a dipolar gain medium," *Nat. Photon.* **4**(6), 382–387 (2010).
11. G. Strangi, A. De Luca, S. Ravaine, M. Ferrie, and R. Bartolino, "Gain induced optical transparency in metamaterials," *Appl. Phys. Lett.* **98**(25), 251912 (2011).
12. A. De Luca, M. P. Grzelczak, I. Pastoriza-Santos, L. M. Liz-Marzán, M. La Deda, M. Striccoli, and G. Strangi, "Dispersed and encapsulated gain medium in plasmonic nanoparticles: a multipronged approach to mitigate optical losses," *ACS Nano* **5**(7), 5823–5829 (2011).

13. D. J. Bergman and M. I. Stockman, "Surface plasmon amplification by stimulated emission of radiation: quantum generation of coherent surface plasmons in nanosystems," *Phys. Rev. Lett.* **90**(2), 027402 (2003).
14. M. C. Gather, K. Meerholz, N. Danz, and K. Leosson, "Spasers explained," *Nat. Photon.* **2**(6), 327–329 (2008).
15. S. Campione, M. Albani, and F. Capolino, "Complex modes and near-zero permittivity in 3D arrays of plasmonic nanoshells: loss compensation using gain," *Opt. Mater. Express* **1**(6), 1077–1089 (2011).
16. C. Argyropoulos, P.-Y. Chen, F. Monticone, G. D'Aguanno, and A. Alù, "Nonlinear plasmonic cloaks to realize giant all-optical scattering switching," *Phys. Rev. Lett.* **108**(26), 263905 (2012).
17. Y. Yang, W. Wang, A. Boulesbaa, I. I. Kravchenko, D. P. Briggs, A. Poretzky, D. Geohegan, and J. Valentine, "Nonlinear Fano-resonant dielectric metasurfaces," *Nano Lett.* **15**(11), 7388–7393 (2015).
18. X. Bian, D. L. Gao, and L. Gao, "Tailoring optical pulling force on gain coated nanoparticles with nonlocal effective medium theory," *Opt. Express* **25**(20), 24566–24578 (2017).
19. D. Gao, R. Shi, Y. Huang, and L. Gao, "Fano-enhanced pulling and pushing optical force on active plasmonic nanoparticles," *Phys. Rev. A* **96**(4), 043826 (2017).
20. K. Kim, H. Lim, and D.-H. Lee, "Invariant imbedding equations for electromagnetic waves in stratified magnetic media: Applications to one-dimensional photonic crystals," *J. Korean Phys. Soc.* **39**(6), L956–L960 (2001).
21. K. Kim, D.-H. Lee, and H. Lim, "Theory of the propagation of coupled waves in arbitrarily inhomogeneous stratified media," *Europhys. Lett.* **69**(2), 207–213 (2005).
22. K. Kim, D. K. Phung, F. Rotermund, and H. Lim, "Propagation of electromagnetic waves in stratified media with nonlinearity in both dielectric and magnetic responses," *Opt. Express* **16**(2), 1150–1164 (2008).
23. D. K. Phung, F. Rotermund, K. Kim, and H. Lim, "Exact calculation of the optical properties of one-dimensional photonic crystals," *J. Korean Phys. Soc.* **52**(5), 1580–1584 (2008).
24. Y. N. Ovchinnikov and I. M. Sigal, "Optical bistability," *J. Exp. Theor. Phys.* **93**(5), 1004–1016 (2001).
25. J. R. Sambles and R. A. Innes, "A comment on nonlinear optics using surface plasmon-polaritons," *J. Mod. Opt.* **35**(5), 791–797 (1988).
26. A. Marini, A. V. Gorbach, D. V. Skryabin, and A. V. Zayats, "Amplification of surface plasmon polaritons in the presence of nonlinearity and spectral signatures of threshold crossover," *Opt. Lett.* **34**(18), 2864–2866 (2009).
27. H. Ikeda, M. Matsuyama, and A. Hasegawa, "Stabilization of dark-soliton transmission by means of nonlinear gain," *J. Opt. Soc. Am. B* **14**(1), 136–143 (1997).

1. Introduction

Nanophotonics is the study of the interaction of light and matter on the subwavelength scale and is a rapidly growing field in nanoscience. Surface plasmon polaritons consist of the light waves trapped on the surface of a medium and the resonant oscillations of surface charges with the light waves. They lead to the enhancement of electromagnetic fields near the surface, thus are suitable for applications in sensor technology [1, 2]. The applications include probing thin films [3], biosensing [4], biological imaging [5] and emerging new areas [6].

Enhanced electromagnetic fields boost nonlinear phenomena around the surface, which are normally too tiny in magnitudes to be investigated. However, it is difficult to see the effect of the surface response in third-order nonlinear processes due to the strong bulk responses. This can be remedied by the excitation of surface plasmons in a system using coupling prisms in the Otto or Kretschmann configuration, where surface plasmon polaritons are excited through attenuated total internal reflection [7]. The prism coupling scheme provides a simple way to enhance the momentum of the incident light, which is required for the excitation of surface plasmons [8]. A similar enhancement of nonlinear responses can be achieved by exciting other wave modes confined near the surface such as slab waveguide modes.

Surface plasmons are usually generated near the frequencies of visible light. As we approach the infrared region, the loss grows rapidly. Recently, it has been shown that active photonic materials are promising in photonics at infrared, ultraviolet and optical frequencies. The gain provided by the emission of a gain medium sustains the electromagnetic wave suffering high attenuation in the metal. It has been demonstrated that it is possible to obtain net gain over losses in a dielectric-metal-dielectric plasmonic waveguide, through an optically pumped layer of fluorescent conjugated polymer adjacent to the metal surface [9].

In addition, gain has directly been measured in a gain medium composed of optically pumped dye molecules, using the long-range surface plasmon-polariton supported by a symmetric metal strip waveguide [10]. Furthermore, recent experiments have observed optical loss compensation

effects in the medium of randomly dispersed nanoshell particles. Coumarin C500 and Rhodamine 6G (R6G) fluorescent dyes were encapsulated into the dielectric shell [11, 12]. It has been shown that metamaterials combined with a gain medium can enhance effective gain due to the strong local field enhancement incurred by metamaterials [13, 14]. There has been a study of metamaterials capable of compensating loss, which are made of a three-dimensional periodic array of nanospheres filled with R6G inside the core [15]. The utility of gain medium has been expanded by employing Fano-resonant coupling between a plasmonic shell and dielectric core, to cloaking and resonant scattering [16], third harmonic generation [17], and optical pulling and pushing [18, 19].

In this paper, we study the interplay between the linear and nonlinear gain effects and the excitation of surface plasmons or a waveguide mode confined at the metal-dielectric boundary or inside the dielectric layer in the Otto configuration. The dielectric material has Kerr-type optical nonlinearity, with a negative imaginary part representing nonlinear gain. We also consider the influence of the negative imaginary part of the linear dielectric permittivity.

Our theoretical method is based on the invariant imbedding method, using which we transform the wave equation into a set of invariant imbedding equations to create an initial value problem. This method is a powerful tool to solve various kinds of singular and nonlinear wave problems [20–23]. We introduce our formalism briefly in the following section.

2. Model and Numerical Method

For a p -polarized wave propagating in a layered structure, the complex amplitude of the magnetic field, $H = H(z)$, satisfies the wave equation

$$\frac{d^2 H}{dz^2} - \frac{1}{\epsilon(z)} \frac{d\epsilon}{dz} \frac{dH}{dz} + [k_0^2 \epsilon(z) - q^2] H = 0, \quad (1)$$

where $k_0 (= \omega/c)$ is the vacuum wave number and ϵ is the dielectric permittivity. When the wave is incident from the region where $z > L$ and $\epsilon = \epsilon_1$ at an angle θ and propagates in the xz plane, $q (= \sqrt{\epsilon_1} k_0 \sin \theta)$ and $p (= \sqrt{\epsilon_1} k_0 \cos \theta)$ are the x and negative z components of the wave vector. We assume the layered structure lies in $0 \leq z \leq L$ and has a Kerr-type nonlinearity in the dielectric permittivity. Then we have

$$\epsilon(z) = \begin{cases} \epsilon_1 & \text{if } z > L \\ \epsilon_L(z) + \alpha(z)|E(z)|^2 & \text{if } 0 \leq z \leq L, \\ \epsilon_2 & \text{if } z < 0 \end{cases}, \quad (2)$$

where $\epsilon_L(z)$ and $\alpha(z)$ are arbitrary complex functions of z . We define the wave function in the incident region as

$$H(z) = v\sqrt{\epsilon_1} \left[e^{ip(L-z)+iqx} + r(L)e^{ip(z-L)+iqx} \right], \quad (3)$$

where $|v|^2 (\equiv w)$ is the intensity of the electric field in the incident wave and r is the reflection coefficient.

We can transform the wave equation into a set of differential equations for the reflection and transmission coefficients, r and t , and the imbedding parameter w using the invariant imbedding method:

$$\begin{aligned} \frac{1}{p} \frac{dr(l)}{dl} &= 2i \frac{\epsilon(l)}{\epsilon_1} r(l) - \frac{i}{2} \left[\frac{\epsilon(l)}{\epsilon_1} - 1 \right] \left[1 - \frac{\epsilon_1}{\epsilon(l)} \tan^2 \theta \right] [1 + r(l)]^2, \\ \frac{1}{p} \frac{dt(l)}{dl} &= i \frac{\epsilon(l)}{\epsilon_1} t(l) - \frac{i}{2} \left[\frac{\epsilon(l)}{\epsilon_1} - 1 \right] \left[1 - \frac{\epsilon_1}{\epsilon(l)} \tan^2 \theta \right] [1 + r(l)] t(l), \\ \frac{1}{p} \frac{dw(l)}{dl} &= \text{Im} \left\{ 2 \frac{\epsilon(l)}{\epsilon_1} - \left[\frac{\epsilon(l)}{\epsilon_1} - 1 \right] \left[1 - \frac{\epsilon_1}{\epsilon(l)} \tan^2 \theta \right] [1 + r(l)] \right\} w(l). \end{aligned} \quad (4)$$

The dielectric permittivity is determined from the cubic equation

$$\epsilon(l) = \epsilon_L(l) + \alpha(l)w(l) \left[\frac{\epsilon_1^2}{|\epsilon(l)|^2} |1 + r(l)|^2 \sin^2 \theta + |1 - r(l)|^2 \cos^2 \theta \right]. \quad (5)$$

Therefore, the invariant imbedding method solves an initial value problem for a system of nonlinear differential equations and the cubic polynomial is solved at each step to evaluate $\epsilon(l)$ inside the structure.

The initial conditions for r , t and w are

$$\begin{aligned} r(0) &= \frac{\epsilon_2 \sqrt{\epsilon_1} \cos \theta - \epsilon_1 \sqrt{\epsilon_2 - \epsilon_1 \sin^2 \theta}}{\epsilon_2 \sqrt{\epsilon_1} \cos \theta + \epsilon_1 \sqrt{\epsilon_2 - \epsilon_1 \sin^2 \theta}}, \\ t(0) &= \frac{2\epsilon_2 \sqrt{\epsilon_1} \cos \theta}{\epsilon_2 \sqrt{\epsilon_1} \cos \theta + \epsilon_1 \sqrt{\epsilon_2 - \epsilon_1 \sin^2 \theta}}, \\ w(0) &= w_0. \end{aligned} \quad (6)$$

The constant w_0 is chosen such that the final solution for $w(L)$ is the same as the physical input intensity. The reflectance R is given by $R = |r(L)|^2$ and the transmittance T is

$$T = \frac{\epsilon_1 \sqrt{\epsilon_2 - \epsilon_1 \sin^2 \theta}}{\epsilon_2 \sqrt{\epsilon_1} \cos \theta} |t(L)|^2. \quad (7)$$

If ϵ is real, there is no loss or gain and the quantities R and T satisfy the law of conservation of energy, $R + T = 1$.

We can also calculate the field distribution inside the medium using the invariant imbedding equation for the normalized magnetic field amplitude $u(z) = H(z)/v$ is given as

$$\frac{1}{p} \frac{\partial u(z, l)}{\partial l} = i \frac{\epsilon(l)}{\epsilon_1} u(z, l) - \frac{i}{2} \left[\frac{\epsilon(l)}{\epsilon_1} - 1 \right] \left[1 - \frac{\epsilon_1}{\epsilon(l)} \tan^2 \theta \right] [1 + r(l)] u(z, l), \quad (8)$$

For a given z ($0 < z < L$), $u(z, L)$ is obtained by integrating this equation, together with the equations for $r(l)$ and $w(l)$, from $l = z$ to $l = L$ using the initial condition $u(z, z) = 1 + r(z)$.

3. Results and Discussion

We are mainly interested in the interplay between the surface confined wave modes and nonlinear gain in the Otto configuration (see Fig. 1). A p wave is incident from a prism onto a nonlinear dielectric-metal bilayer, which lies on a dielectric substrate. We assume that both the prism and the substrate have refractive indices of 1.77 and the dielectric permittivity of the nonlinear dielectric layer is given by

$$\epsilon = \epsilon_a + i\gamma + (\alpha + i\beta) |\mathbf{E}|^2. \quad (9)$$

We note that both the linear part of the permittivity and the third-order nonlinear optical susceptibility are complex quantities. We choose $\epsilon_a = 1.46^2 = 2.1316$. The wavelength of the incident wave is 633 nm and the dielectric permittivity of the metal layer is $-16 + i$ corresponding to silver at that wavelength. The thicknesses of the nonlinear dielectric and metal layers are 320 nm and 50 nm. Positive (negative) values of γ and β correspond to linear and nonlinear losses (gains) respectively. The critical incident angle θ_c in the linear case is equal to 55.57° .

We first consider the situation where there is only linear gain. In Fig. 2, we plot the reflectance R versus incident angle θ for different values of the linear gain coefficient γ when $\alpha = \beta = 0$. In Fig. 2(a), we find that the influence of linear gain is small when $|\gamma| \leq 0.01$, since the reflectance

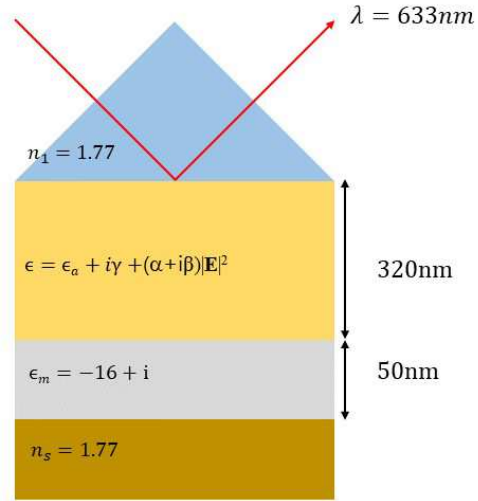


Fig. 1. Schematic of the Otto configuration.

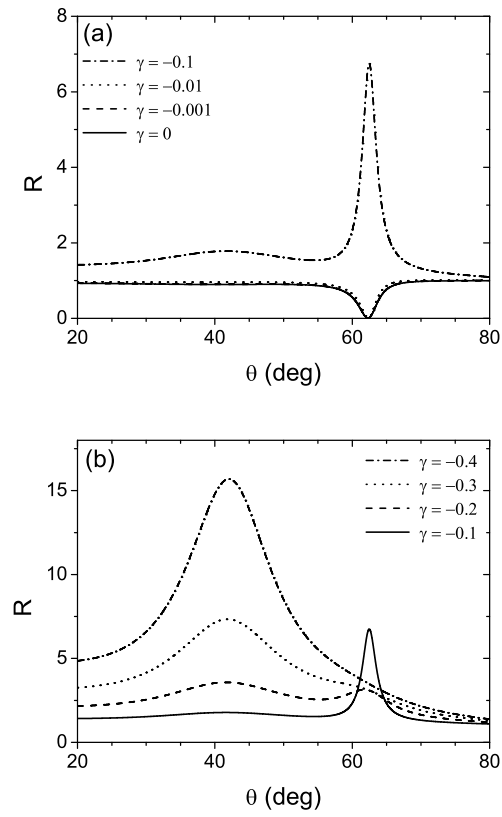


Fig. 2. Reflectance vs. incident angle for various values of the linear gain coefficient γ when $\alpha = \beta = 0$. (a) $\gamma = 0, -0.001, -0.01, -0.1$, (b) $\gamma = -0.1, -0.2, -0.3, -0.4$.

curves do not show much appreciable change. There is a dip in R due to the excitation of surface plasmons at $\theta = 62.285^\circ$ for $\gamma = 0$ and at $\theta = 62.29^\circ$ for $\gamma = -0.0001$ and -0.01 . When $\gamma = -0.1$, the reflectance shows a peak rather than a dip at $\theta = 62.47^\circ$ with the peak value ($R \approx 6.75$) much larger than 1. Thus the reflected power is larger than the incident power. This over-reflection signifies the amplification of the wave energy due to the interplay between the excitation of surface plasmons and the linear gain effect. We also find that a new broad peak with the peak value of $R \approx 1.781$ occurs around $\theta = 41.61^\circ$. This peak is due to the interplay between a waveguide mode inside the dielectric layer and linear gain.

In Fig. 2(b), we show the results for larger values of the gain coefficient $|\gamma|$. We find that as $|\gamma|$ increases, the peak associated with surface plasmon excitation (around $\theta = 62^\circ$) gradually decreases away, while the peak associated with a waveguide mode (around $\theta = 42^\circ$) gets strongly enhanced. We can see clearly that there are two peaks when $\gamma = -0.2$. When $\gamma = -0.4$, R reaches 15.6867 at $\theta = 42.025^\circ$. Since this angle is smaller than θ_c , refracted waves can propagate inside the dielectric layer.

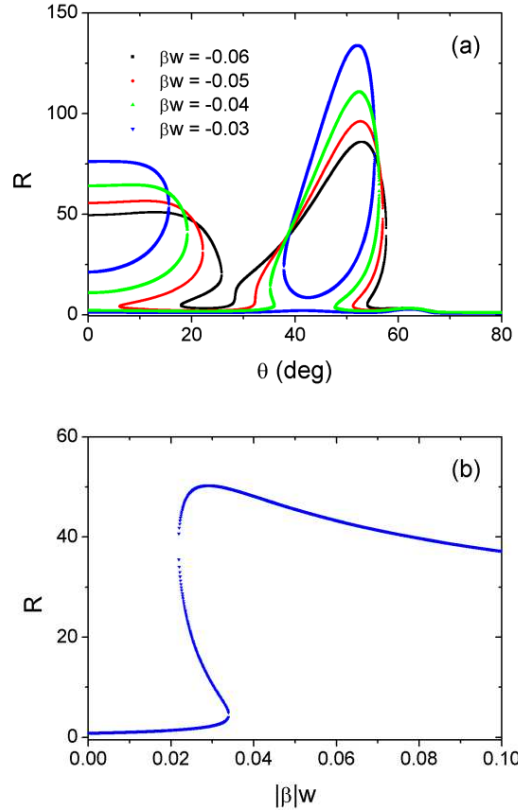


Fig. 3. (a) Reflectance vs. incident angle for various values of the nonlinear gain coefficient βw and (b) reflectance vs. nonlinear gain coefficient $|\beta|w$ for the incident angle $\theta = 40^\circ$, when $\gamma = 0$ and $\alpha = 0$.

Next, we consider the influence of nonlinear gain. A proper dimensionless parameter measuring the strength of the nonlinear gain effect is βw , where w is the intensity of the incident wave. For now, we turn off γ and α and focus on the effect of βw . In Fig. 3(a), we plot the reflectance versus incident angle for various values of the nonlinear gain parameter βw . As $|\beta|w$ is reduced from 0.06, the solution curve displaying multistability goes through

successive deformation. For $\beta w = -0.03$, the curve has three separate parts, one of which is a closed curve located between $\theta \approx 38^\circ$ and $\theta \approx 55^\circ$. We can distinguish the stable solutions from the unstable ones by plotting the reflectance versus βw . In Fig. 3(b), we show the reflectance curve for $\theta = 40^\circ$ when the nonlinear gain parameter $|\beta|w$ is varied. We notice that there is a region where there exist three solutions for a given value of $|\beta|w$. It is well-known that nonlinear resonance problems have multiple solutions with alternating stable and unstable branches for a given intensity of incident light [24]. The unstable branch is located between the stable branches at its bottom and top positions. This is a usual mechanism for hysteresis. The change in the number of multistable solutions for varying θ is not monotonic.

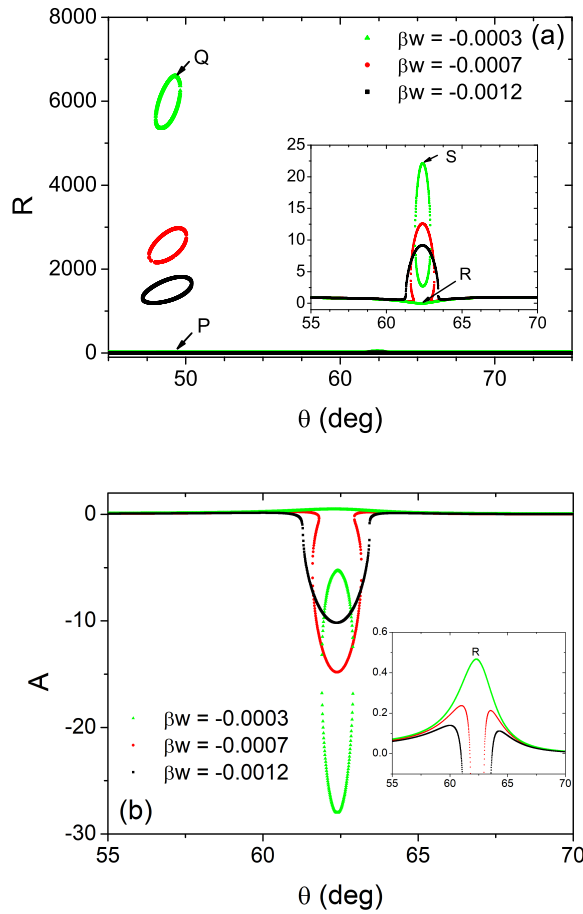


Fig. 4. (a) Reflectance R and (b) absorptance A plotted vs. incident angle for various values of the nonlinear gain coefficient βw , when $\gamma = 0$ and $\alpha = 0$. Insets: the expanded view of some parts of each plot.

In Fig. 4(a), the reflectance curves for smaller values of $|\beta|w$ are shown. The values of R become very large, reaching about 6601 for $\beta w = -0.0003$. In the range of the incident angle where such huge amplification takes place, a propagating wave travels inside the dielectric layer. Our explanation about the possible physical mechanism will be given in the discussion of Fig. 5 later.

In the inset of Fig. 4(a), the curves around $\theta = 62.28^\circ$ are expanded to show their behavior in

detail. In this range of the incident angle, an evanescent wave is amplified through the excitation of surface plasmons. When $\beta w = -0.0007$, the reflectance takes a local maximum around $\theta = 62.28^\circ$. Since the curve is deformed to form a partial loop (in the shape of Ω) around this angle, there are two optical bistability regions, which occur in the small ranges of incident angles in $61.6^\circ - 61.81^\circ$ and $62.95^\circ - 63.17^\circ$. When the incident angle goes through these regions of optical bistability, the reflectivity jumps up from a small to a larger value, or vice versa. When the nonlinear gain parameter is about -0.0012 , the optical bistability cannot be observed and the maximum of the reflectance is smaller than the value in the previous case where the nonlinear gain parameter is about -0.0007 .

In Fig. 4(b), we plot the absorptance $A (= 1 - R - T)$. In most of our calculations, A is negative due to the fact that R and T are greater than 1. In the inset of Fig. 4(b), the plot is expanded around $A = 0$. At the point R corresponding to $\theta = 62.29^\circ$, $A \approx 0.467 > 0$ when $\beta w = -0.0003$. This case corresponds to the point R in Fig. 4(a), where R and T are less than 1. When $|\beta|w \ll 1$, the electromagnetic fields associated with the surface plasmon are weak and confined close to the nonlinear dielectric-metal interface. Because of this, the damping effect due to the metal layer can be bigger than the amplification effect due to the dielectric layer and we have $0 < A < 1$. As $|\beta|w$ increases, the surface plasmon fields have bigger amplitude and the amplification effect dominates metallic damping, resulting in $A < 0$ [see Fig. 5(b)]. Therefore, as the incident intensity w is increased up and decreased down [see Fig. 3(b)], the system makes a transition between damping and amplification. This may lead to a new device which allows a system to have a self-control to prevent thermal damage.

In Fig. 5, we show the magnetic field profiles corresponding to the points P, Q, R and S indicated in Fig. 4(a). In Fig. 5(a), the first solution (P) and the third solution (Q) at $\theta = 49.32^\circ$ are shown. In the inset of Fig. 5(a), an expanded view of the first solution is shown. The third solution is amplified strongly near the input side. As we have seen in Fig. 2, this resonance occurs at incident angles less than the critical angle in a medium with strong gain. Nonlinear gain is not homogeneous in the medium due to the inhomogeneous electric field. When a light with high intensity is incident on the system, the refractive index near the input side will increase, thus the propagating waves are reflected before reaching the other end. Hence in order to obtain strong enhancement, the nonlinear gain must not be too high.

The situation in Fig. 5(a) shows that some sort of Fabry-Perot cavity is formed in the dielectric layer, where propagating waves travel between the input face and the metal-dielectric interface. This will lead to strong amplification. As the local field is enhanced, the nonlinear gain βw gets larger, resulting in the growth of resonance. Such enormous enhancement looks promising, but the high electric field boosted by three orders of magnitude may cause damage in the thin dielectric or metal film due to Joule heating [25] even in the Otto configuration. In Fig. 5(b), the first solution corresponds to the point R, which is the point where the damping ($A > 0$) takes the maximum value shown in the inset of Fig. 4(b) at $\theta = 62.29^\circ$.

So far we have considered the effects of the gain parameters γ and βw separately. Now we consider the case where the dielectric layer has both focusing nonlinearity and nonlinear gain. In Fig. 6(a), we plot the reflectance versus incident angle for several values of γ , when $\alpha w = 0.0028$ and $\beta w = -0.0028$. For all values of γ , there are two closed solution curves with very large R around $\theta = 40^\circ$ and $\theta = 62^\circ$. In addition, there exist solutions with much smaller values of R in the interval $55^\circ < \theta < 70^\circ$, which are shown in the inset. The optical bistability can be observed in this case when $|\gamma| < 0.1$. When $\gamma = -0.1$, no optical bistability is observed. It appears that the self-focusing nonlinearity αw quenches the amplification effect due to the linear and nonlinear gain, while multistability occurs in a wider range of the incident angle. It is well-known that Kerr-type nonlinearity can induce severely multistable solutions [22]. The reflectance and the transmittance change substantially for a very small change of the nonlinearity parameter αw and the field profiles inside the system are highly nonuniform. When the focusing nonlinearity

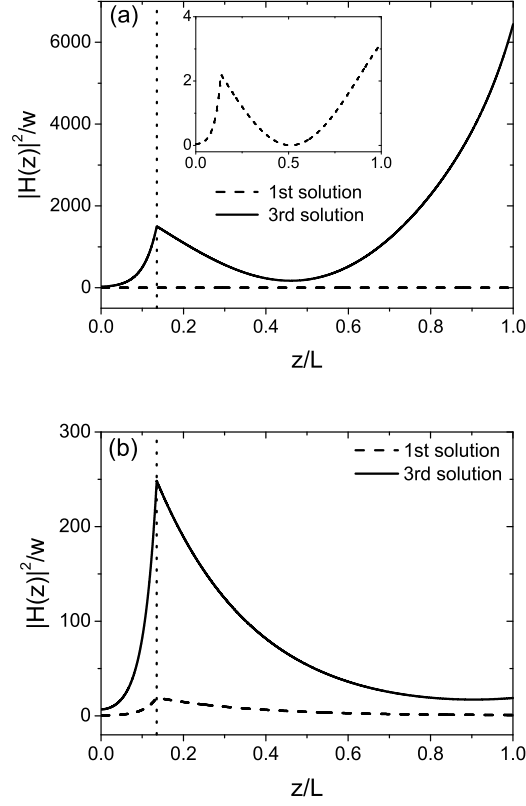


Fig. 5. Normalized field profiles inside the metal/dielectric bilayer of thickness L ($= 370$ nm) at the points P, Q, R and S indicated in Fig. 4(a). (a) 1st solution (point P) and 3rd solution (point Q) at $\theta = 49.32^\circ$. Inset: the expanded view of the 1st solution. (b) 1st solution (point R) and 3rd solution (point S) at $\theta = 62.29^\circ$. The vertical dotted line indicates the position of the metal/dielectric boundary. The wave is incident from $z > L$ onto the dielectric layer side.

is turned on in Fig. 6, the propagating waves in the dielectric layer encounter inhomogeneous fields varying in a complicated manner, even for a small change in the input intensity. Thus the Fabry-Perot-type amplification as in Fig. 5(a) does not occur, as is evident in Fig. 6(b). Such complex landscape of fields would also degrade the propagation of surface plasmons. If we reduce the strength of nonlinear gain such that $\alpha w = 0.0028$ and $\beta w = -0.0007$, the influence of αw becomes stronger and amplification is greatly reduced. We observe that complicated patterns of multistability appear in this case. When $\gamma = -0.1$, no multistability is observed.

In a saturable nonlinear gain medium, saturation occurs when the amplification of surface plasmon polaritons is compensated by the nonlinear losses [26]. In this case, taking the saturation effect into account, the dielectric constant may be written as

$$\epsilon = \epsilon_L + \frac{\alpha_s |\mathbf{E}|^2}{1 + \beta_s |\mathbf{E}|^2}, \quad (10)$$

where ϵ_L is the linear part and α_s and β_s are the coefficients for the nonlinear term. For $\beta_s \ll 1$, it can be approximated to

$$\epsilon \approx \epsilon_L + \alpha_s |\mathbf{E}|^2 - \alpha_s \beta_s |\mathbf{E}|^4. \quad (11)$$

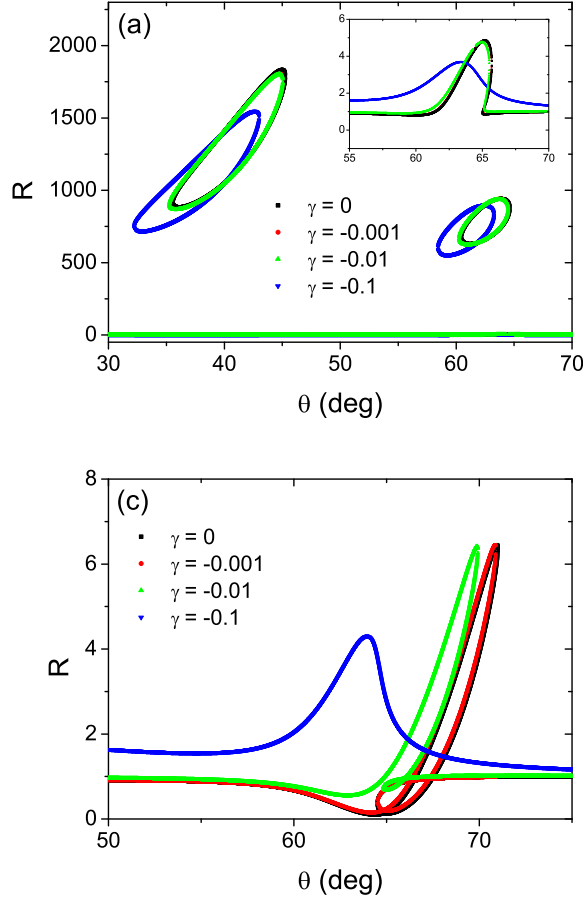


Fig. 6. Reflectance vs. incident angle for various values of the linear gain coefficient γ , when (a) $\alpha w = 0.0028$ and $\beta w = -0.0028$, (b) $\alpha w = 0.0028$ and $\beta w = -0.0007$. Inset: the expanded view of some part of (a).

Thus a higher order term with the opposite sign to the Kerr-nonlinear term appears, introducing loss. Under this condition, the field enhancement on the boundaries of the dielectric layer should be limited. On the other hand, our model does not have loss built inside since it is in the form $\epsilon = \epsilon_L + \alpha|\mathbf{E}|^2$. However, the Fabry-Perot-type amplification in Fig. 5(a) has its own limit, because the field in the middle of the dielectric layer cannot grow faster than the field at the boundaries. Thus as $|\beta|w$ grows, the amplification is reduced.

In order to observe the effects discussed in this paper, we have found that we need to have the nonlinear gain parameter $|\beta|w$ in the order of magnitude of 10^{-4} . We point out that systems with large nonlinear gain parameters have been studied in the area of soliton transmission in fibers [27]. Though we do not currently have a realistic model relating the nonlinear gain parameter with material dielectric functions, we speculate that it may be possible to fabricate systems with large nonlinear gain by combining materials with large Kerr coefficients and gain media, using the scheme of metamaterials research.

4. Conclusion

In this paper, we have studied the interplay between the surface confined wave modes such as surface plasmons and waveguide modes and the linear and nonlinear gain effects in the Otto configuration. In the linear case, we have found that a large reflectance peak is generated due to this interplay and the incident angle at which the peak occurs shifts from the angle associated with surface plasmons to that associated with a waveguide mode, as the gain parameter increases. When the nonlinear gain is nonzero, we have found that there appear strong multistability phenomena near the incident angles associated with surface plasmons and a waveguide mode. We have shown that the reflectance curve can display topologically complicated multistability structure. When the nonlinear gain parameter takes a small optimal value, we have found that a giant amplification of the reflectance by three orders of magnitude can occur near the incident angle associated with a waveguide mode. We have also found that there exists a range of the incident angle where the wave is dissipated in the presence of gain and suggested that this can provide a possible new technology for thermal control in the subwavelength scale.

Funding

National Research Foundation of Korea Grant funded by the Korean Government (NRF-2015R1A2A2A01003494).